



Dalton
Transactions

14-electron Rh and Ir silylphosphine complexes and their catalytic activity in alkene functionalization with hydrosilanes

Journal:	<i>Dalton Transactions</i>
Manuscript ID	DT-ART-03-2021-000677.R1
Article Type:	Paper
Date Submitted by the Author:	05-Jul-2021
Complete List of Authors:	Abeynayake, Niroshani; Mississippi State University, Chemistry Zamora-Moreno, Julio ; Universidad Autonoma del Estado de Morelos Gorla, Saidulu; Mississippi State University, Chemistry Donnadieu, Bruno; National University of Singapore, Department of Chemistry Muñoz, Miguel; Mississippi State University, Chemistry Department Montiel-Palma, Virginia; Mississippi State University, Chemistry

SCHOLARONE™
Manuscripts

ARTICLE

14-electron Rh and Ir silylphosphine complexes and their catalytic activity in alkene functionalization with hydrosilanes

Niroshani S. Abeynayake,^a Julio Zamora-Moreno,^{a,b} Saidulu Gorla,^a Bruno Donnadieu,^a Miguel A. Muñoz-Hernández^{*a} and Virginia Montiel-Palma^{*a}

Received 00th January 20xx,
Accepted 00th January 20xx

DOI: 10.1039/x0xx00000x

Herein we report an experimental and computational study of a family of four coordinated 14-electron complexes of Rh(III) devoid of agostic interactions. The complexes $[X\text{-Rh}(\kappa^3\text{-P,Si,Si})\text{PhP}(\text{o-C}_6\text{H}_4\text{CH}_2\text{Si}^i\text{Pr}_2)_2]$, where X = Cl (**Rh-1**), Br (**Rh-2**), I (**Rh-3**), OTf (**Rh-4**), Cl-GaCl₃ (**Rh-5**); derive from a bis(silyl)-*o*-tolylphosphine with isopropyl substituents on the Si atoms. All five complexes display a sawhorse geometry around Rh and exhibit similar spectroscopic and structural properties. The catalytic activity of these complexes and $[\text{Cl-Ir}(\kappa^3\text{-P,Si,Si})\text{PhP}(\text{o-C}_6\text{H}_4\text{CH}_2\text{Si}^i\text{Pr}_2)_2]$, **Ir-1**, in styrene and aliphatic alkene functionalizations with hydrosilanes is disclosed. We show that **Rh-1** catalyzes effectively the dehydrogenative silylation of styrene with Et₃SiH in toluene while it leads to hydrosilylation products in acetonitrile. **Rh-1** is an excellent catalyst in the sequential isomerization/hydrosilylation of terminal and remote aliphatic alkenes with Et₃SiH including hexene isomers, leading efficiently and selectively to the terminal anti-Markonikov hydrosilylation product in all cases. With aliphatic alkenes, no hydrogenation products are observed. Conversely, catalysis of the same hexene isomers by **Ir-1** renders allyl silanes, the tandem isomerization/dehydrogenative silylation products. A mechanistic proposal is made to explain the catalysis with these M(III) complexes.

Introduction

The quest for the synthesis and isolation of elusive unsaturated transition metal complexes has been for years motivated by their involvement in crucial catalytic and fundamental processes. Unsaturated 14-electron species of Rh and Ir exist either as three-coordinated T-shaped M(I)¹⁻⁴ or as four-coordinated⁵⁻¹⁰ M(III) complexes (**Chart 1**). These exotic species are generally stabilized by agostic interactions, intramolecular hemilabile bonds or secondary π contacts and in general by bulky ligands on the transition metal center. We recently reported facile access to rare Rh and Ir(III) 14-electron species $[\text{Cl-M}(\kappa^3\text{-P,Si,Si})\text{PhP}(\text{o-C}_6\text{H}_4\text{CH}_2\text{Si}^i\text{Pr}_2)_2]$ (M = Rh, **Rh-1** and M = Ir, **Ir-1**)¹¹ and $[\text{MeIr}(\kappa^3\text{-P,Si,Si})\text{PhP}(\text{o-C}_6\text{H}_4\text{CH}_2\text{Si}^i\text{Pr}_2)_2]$.¹² Complexes **Rh-1** and **Ir-1** result from the reaction of $[\text{MCl}(\text{COD})_2]$ and the isopropyl substituted pincer-like *Si,P,Si* ligand. The analogous methyl substituted ligand gives rise to dimeric 16-electron Rh and Ir species.¹³ We now report the structural and spectroscopic characterization of the family of 14-electron complexes resulting from substitution reactions on

complex **Rh-1**. None of these complexes exhibits significant agostic interactions. Additionally, their catalytic activity in hydrosilylation/dehydrogenative silylation of alkenes is presented.

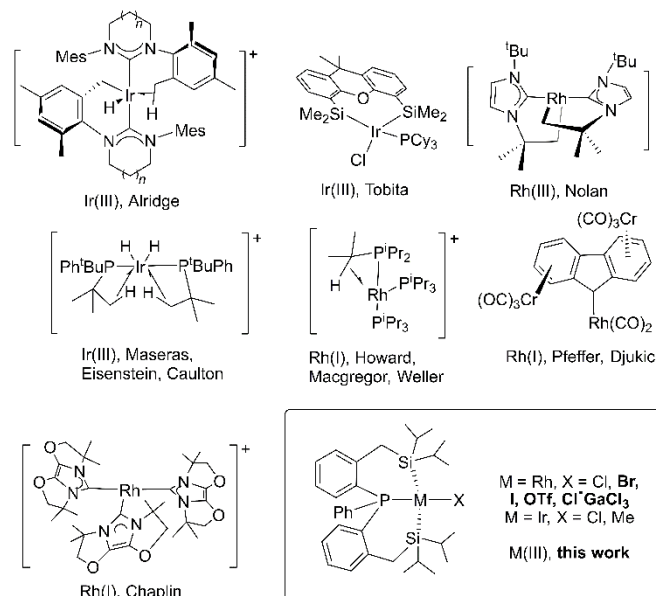


Chart 1. Reported 14-electron Rh and Ir complexes.

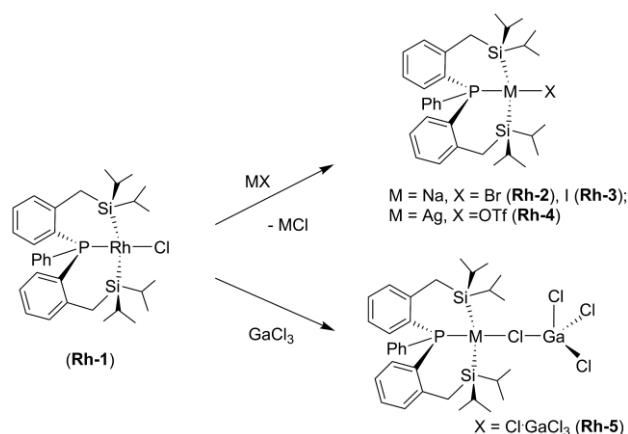
Results and Discussion

1. Synthesis and characterization of a family of 14-electron rhodium complexes: Rh-2, Rh-3, Rh-4 and Rh-5. To access complexes closely related to **Rh-1**, we carried out the exchange

^a Department of Chemistry, Mississippi State University, Box 9573, Mississippi State, Mississippi 39762, United States. E-mails: mmunoz@chemistry.msstate.edu and vmontiel@chemistry.msstate.edu

^b Centro de Investigaciones Químicas-ICBA, Universidad Autónoma del Estado de Morelos, Av. Universidad 1001, Col. Chamilpa, Cuernavaca, Morelos 62209, Mexico

Electronic Supplementary Information (ESI) available: Full experimental details of the synthesis of all compounds including NMR spectra and X Ray diffraction data of complexes **Rh-2**, **Rh-3**, **Rh-4**, **Rh-5** (CCDC 2031071-2031074) as well as theoretical calculations details and optimizations. Full catalysis tables and NMR spectra of catalytic reactions. Text files of all computed molecule Cartesian coordinates are provided in a format for convenient visualization. See DOI: 10.1039/x0xx00000x



Scheme 1. Synthetic route to the family of 14-electron complexes of **Rh-1**.

of the chloride in **Rh-1** by other X type ligands (I^- , Br^- , OTf^-). Solutions of complex **Rh-1** were reacted with the corresponding sodium or silver salts (**Scheme 1**). The 14-electron Rh complexes of general formula $[\text{XRh}(\kappa^3(\text{P}, \text{Si}, \text{Si})\text{PhP}(\text{o}-\text{C}_6\text{H}_4\text{CH}_2\text{Si}(\text{Pr})_2)_2)]$ ($X = \text{Br}$, **Rh-2**; I , **Rh-3**; OTf , **Rh-4**), depicted in **Scheme 1**, were synthesized in good isolated yields. Aiming at the formation of a cationic species by removal of the chloride ligand, addition of GaCl_3 to **Rh-1** was performed. The resulting complex incorporates GaCl_3 as the $\mu\text{-Cl}$ adduct **Rh-5**, also a 14-electron species. New complexes **Rh-2**, **Rh-3**, **Rh-4** and **Rh-5** were fully characterized in solution by spectroscopic techniques, in the solid state by single crystal X ray diffraction and by theoretical means. Their ^{31}P ^{14, 15} spectra show a doublet signal due to coupling of the ^{31}P nucleus with ^{103}Rh in a chemical shift between 30.9 ppm $< \delta < 37.7$ ppm and with coupling constants $^1J_{\text{P-Rh}}$ between 147 Hz $< ^1J_{\text{P-Rh}} < 178$ Hz. These values are close to those found in the parent **Rh-1** (δ 31.07, $^1J_{\text{P-Rh}} = 147$ Hz),¹¹ indicating close similarities between all the species (Table 1).

The X-ray diffraction structures of **Rh-2**, **Rh-3**, **Rh-4** and **Rh-5** are gathered in Figure 1. In the solid state, all complexes exhibit very similar structural parameters. In all, the geometry around the Rh center is best described as a distorted sawhorse. The X-Rh bond distances gradually expand in the halogen series **Rh-1** according to the larger ionic radii of X. The X-Rh-P angles show small variations from those in **Rh-1**. Direct comparison of the structures of **Rh-5** and **Rh-1** shows an elongation of the Rh-Cl

bond distance in **Rh-5** in comparison with **Rh-1** due to it bonding an additional metal.

Analysis of the bond distances/contacts in all structures show there are no short enough H...Rh/C...Rh contacts to support the presence of significant agostic interactions to account for the stabilization of the molecules.^{16, 17}

Remarkably, except the GaCl_3 adduct **Rh-5**, all the new complexes are air-stable in the solid state. This behavior is in contrast with our previously reported findings in dinuclear species $[\text{Cl-M}(\kappa^3(\text{P}, \text{Si}, \text{Si})\text{PhP}(\text{o}-\text{C}_6\text{H}_4\text{CH}_2\text{SiMe}_2)_2)_2]$ bearing methyl substituents on the Si atoms.¹³

The reactivity of **Rh-1** towards 2-electron donor ligands also led to significant differences. Attempted reactions of **Rh-1** with PCy_3 , PPh_3 and $\text{P}(\text{OPh})_3$ do not lead to the observation of any new product. In contrast, the closely related Ir(III) dimer $[\text{Ir}(\kappa^3(\text{P}, \text{Si}, \text{Si})\text{PhP}(\text{o}-\text{C}_6\text{H}_4\text{CH}_2\text{SiMe}_2)_2)_2]$ undergoes an equilibrium in solution with its monomer and reacts with phosphine ligands at room temperature incorporating one equivalent of bulky PPh_3 or PCy_3 .¹⁸ It could be argued that the bulkier isopropyl substituents on Si do not allow for the formation of 16-electron species due to steric constraints.¹¹ No conclusive evidence for the formation of an acetonitrile adduct of **Rh-1** was obtained even in pure CH_3CN solutions. Reaction of **Rh-1** with excess Et_3SiH (1:100 molar ratio) does not occur but in the presence of excess styrene (1:10), a styrene adduct is detected by NMR spectroscopy.

Next, we turned to theoretical computations to gain understanding of the frontier molecular orbitals of the Rh complexes.

2. DFT calculations. The optimized DFT structures of complexes **Rh-1**, **Rh-2**, **Rh-3**, **Rh-4** and **Rh-5** were computed in the gas phase with method $\text{wB97XD}/6\text{-31g}(\text{d})$ on C, H, Cl, P, Si and $\text{wB97XD}/\text{SDD}$ on Br, Ga, I, Rh as detailed in the ESI. In the first place, NBO natural charges (Table S1) show a steady increase in the negative charge on the Rh atom (-0.72 in **Rh-1**, -0.78 in **Rh-2** and -0.88 in **Rh-3**) upon going from Cl to Br or I, consistent with electronegativity values. As expected, comparison of the Rh charges on **Rh-1** and **Rh-5** shows a larger negative value in **Rh-1** (-0.72) than in **Rh-5** (-0.58) attributed to the larger ionic pair character in the latter.

Table 1. Comparison of structural (XRD at 100K) and NMR spectroscopic parameters (C_6D_6 , 298 K) of 14-electron Rh complexes.

Parameter	Rh-1 (X= Cl)	Rh-2 (X= Br)	Rh-3 (X= I)	Rh-4 (X= OTf)	Rh-5 (X= ClGaCl ₃)
X-Rh / Å	2.314(2)	2.4349(5)	2.6004(2), 2.5924(2)	2.1736(14)	2.4243(6)
X-Rh-P / °	164.45(8)°	164.243(19)°	161.285(18)°	170.27(4)°	167.509(17)
δ $^{31}\text{P}\{\text{H}\}$ / ppm (C_6D_6)	31.1	31.8	30.9	37.7	34.8
$^1J_{\text{P-Rh}}$ / Hz	147	149	147	170	178

We attribute the remarkable stability experimentally observed in complexes **Rh-1** to **Rh-4** to the combination of the electronic stabilization provided by the two excellent σ -donor Si atoms on the bis(silyl)phosphine ligand enhancing the electron density at the Rh center, the large HOMO-LUMO gap (Table S2, ESI), and the steric protection of the bulky isopropyl substituents on the Si atoms.

3. Catalytic activity in alkene dehydrogenative silylation. 3.1.

Styrene and derivatives. Silylation, including hydrosilylation, of internal alkenes is more challenging than that of terminal olefins, yet it is critical because isomeric mixtures of alkenes are more readily accessible than pure terminal olefins. Homogeneous molecular systems based on Fe,¹⁹ Co,²⁰⁻²³ Ni,^{24, 25} Rh²⁶ and Ir^{27, 28} as well as Ni and Co²⁹ nanoparticles¹² are known to achieve internal alkene silylations through sequential isomerization-hydrosilylation.^{21, 30} A few of these systems require large metal loadings, dual catalysts, additives, harder reaction conditions, or secondary alkylsilanes.²⁸

In parallel, the selective and efficient transformation of organosilanes to double functionality vinyl- and allyl silanes, is a treasured reaction because the products are versatile building blocks used as final products and as monomers for polymerizations in the plastic and fine chemical industries.^{31,32 33-35} Amongst the current synthetic methods for their synthesis, alkene dehydrogenative silylation is one of the most desired routes. This is partly due to the lower cost of alkenes as starting materials in comparison with the corresponding alkynes for direct hydrosilylation. Xie and Zhang have recently disclosed the direct synthesis of the dehydrogenative silylation products of styrene, **1**, and Et₃SiH to triethyl(styryl)silane, **2**, from the use of [RhCl(COD)]₂ and excess PPh₃ as the catalytic system (Equation 1).³⁶

We also examined the rhodium complexes **Rh-1**, **Rh-2**, **Rh-3**, **Rh-4**, **Rh-5** and the iridium species **Ir-1** as catalysts in the above reaction. As expected, in addition to the hydrogenation product ethylbenzene, employment of Rh or Ir complexes as catalysts afforded a mixture of dehydrogenative silylation/hydrosilylation products (**2/3**) in various ratios when using toluene, dichloromethane or THF as solvents (Tables 2, S3 and S4). Our catalysts are also highly regioselective to the *E*-stereoisomer triethyl(styryl)silane, **2**, as the dehydrogenative silylation product. Optimization of the catalytic conditions including addition of a sacrificial hydrogen acceptor, considerably enhances the selectivity of the catalytic system towards **2** (Table 2 and Table S3) to a 90:10 ratio when employing **Rh-1** and to 80:20 (Table S4) with **Ir-1** as catalyst.

In the absence of sacrificial hydrogen acceptors and under the same conditions (solvent, temperature), there is little variation in the catalytic activity of the Rh complexes **Rh-1**, **Rh-2** and **Rh-3**, except in the case of the triflate complex **Rh-4**, which is more selective towards the hydrosilylation product **3** disfavoring the formation of the unsaturated product (Table 2 and Table S3). The preference of **Rh-4** for hydrosilylation with respect to dehydrogenative silylation (in a 3:1 ratio) could be explained by the influence of the triflate moiety³⁷ which in solution could adopt different coordination modes to Rh including κ^1 and κ^2 ,³⁷⁻³⁹ therefore modifying its ability to coordinate styrene and

undergo the proposed transformation (Scheme 2). The

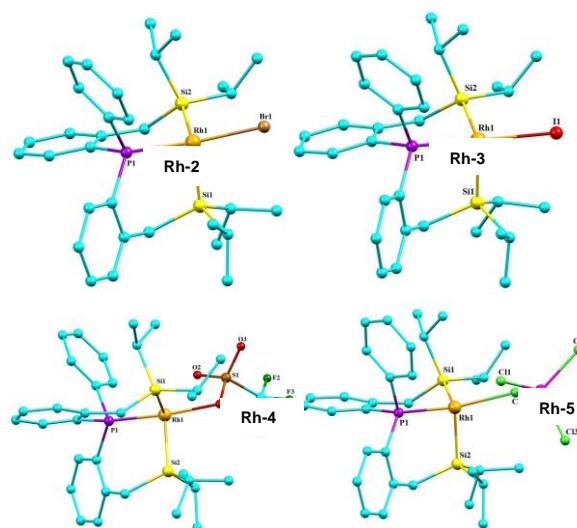


Figure 1. X-Ray structures of complexes **Rh-2**, **Rh-3**, **Rh-4** and **Rh-5**, all showing sawhorse geometries. Ellipsoids are shown at 50% probability. All hydrogen atoms have been omitted for clarity. Important distances (Å) and angles (°) as follows. **Rh-2**: Rh-Br 2.4349(5), Br-Rh-Si1 89.05(2), Br-Rh-Si2 102.429(19), P-Rh-Br 164.243(19), Si2-Rh-Si1 100.11(2). **Rh-3**: Rh-I 2.6004(2), I-Rh-Si1 100.115(18), I-Rh-Si2 108.071(18), P-Rh-I 161.285(18), Si2-Rh-Si1 98.97(2). **Rh-4**: Rh-O 2.1736(14), O-Rh-Si1 96.28(4), O-Rh-Si2 98.17(4), P-Rh-O 170.27(4), Si2-Rh-Si1 97.82(2). **Rh-5**: Rh-Cl 2.4243(6), Cl-Rh-Si1 97.01(2), Cl-Rh-Si2 101.46(2), P-Rh-Cl 167.509(17), Si2-Rh-Si1 99.265(18).

catalytic performance in hydrosilylation is enhanced when a bond to a ligand's oxygen atom is established in recently reported NHCs Rh complexes.²⁶ Hemilability of O- and N- atoms affects the catalysis outcome and product distribution.⁴⁰⁻⁴² We postulate the enhanced selectivity towards hydrosilylation in the triflate system is due to the involvement of a κ^2 coordination mode.

The catalytic activity of **Rh-5** could not be verified in toluene due to its low solubility, however, in dichloromethane as solvent, the ratio **2/3** is similar to that in the series **Rh-1**, **Rh-2**, **Rh-3**. In contrast, the hydrogenation product ethylbenzene (Table S3), increases in comparison to the halogen catalysts and is similar to that found upon catalysis with **Rh-4**. The possibility of the GaCl₄⁻ moiety attaining a κ^2 coordination mode⁴³ is also invoked to explain these findings. Additionally, it is known that the selectivity of cationic Rh species is sometimes opposite to that of their neutral counterparts as seen in the catalyzed hydrosilylation of 1-alkynes by neutral RhCl(PPh₃)₃ and or [Rh(1,5-COD)₂]⁺/PPh₃ which exhibit opposite stereoselectivity.⁴⁴ However, other systems show little variations upon forming a related cationic species.²⁶

From Table 2 (and S3) it is evident that in our system, styrene is more effective than norbornene for steering the selectivity towards the dehydrogenative silylation product. Several studies have evaluated the effectiveness of sacrificial hydrogen acceptors, SHA, including strained bicyclic alkenes such as norbornene, to improve the yield of dehydrogenative silylation over hydrosilylation. For example, in the Ru alkylidene

catalyzed reaction of styrene and alkyl- or alkoxy silanes there is a correlation of the ring strain of the SHA with increased selectivity towards the dehydrogenative silylation product.⁴⁵

In contrast, our results show a competitive coordination of norbornene with styrene, the first required step in the proposed reaction mechanism (**Scheme 2**). Previous studies that have demonstrated that the selectivity to dehydrogenative silylation is also highly affected by the ratio of the substrate/silane.⁴⁶ For example, Murai demonstrated that dehydrogenative silylation of 1,5-hexadiene was selective when using an excess of 1,5-hexadiene/hydrosilane ratio.⁴⁷ From the proposed mechanistic cycles (Scheme 2 and Scheme 3), it can be inferred that excess silane favors hydrosilylation while excess styrene leads to the dehydrogenative silylation or hydrogenation products.

We found that substituents in the *para* position of styrene (Me, ^tBu, ^tBuO, Cl, CF₃) are well tolerated by **Rh-1** and afford dehydrogenative silylation products with excellent selectivity under optimized conditions in toluene (Table 3). Notably, conversion of the tert-butyl substituted styrene showed a selectivity 93:7 when catalyzed by **Rh-1**. Conversion and selectivity are lower when employing **Ir-1**, also manifested in longer reaction times (Table 3).

Scheme 2 shows the mechanistic proposal which incorporates our findings. Given that our catalysts are formally M(III), addition of HSiEt₃ does not lead to the oxidative addition product as we have corroborated in stoichiometric studies. However, we proposed styrene coordination and formation of species A triggers the formation of the silyl species B in which migratory insertion to C is possible. Intermediate C can either undergo β-hydrogen elimination to D and render the triethyl(styryl)silane product **2**. Coordination of a further styrene molecule would lead to ethylbenzene upon hydride migratory insertion from E. Alternatively, species C can lead to the hydrosilylated product **3** and regeneration of B upon reaction with HSiEt₃ and styrene. This proposal also explains the experimental observation that excess Et₃SiH favors hydrosilylation while excess styrene steers the reaction towards **2** (Scheme S1).

3.2 Other alkenes. Other aliphatic and aromatic alkenes also undergo transformation when catalyzed by **Rh-1** or **Ir-1** in toluene. Most notably, remote alkenes are also selectively transformed by our catalysts.

We found that **Rh-1** catalyzes the hydrosilylation of several hexene isomers, 1-octene, 3,3-dimethylbutene and allylbenzene providing the products in good yields with high selectivities (Tables 4 and S5). For example, the reaction of 1-hexene with Et₃SiH afforded the hydrosilylated product with 99% selectivity.

The conversion of internal hexenes to the same linear hydrosilylated product is also efficiently achieved by **Rh-1**. Indeed, the hydrosilylation of internal alkenes *trans-2*, *trans-3*, *cis-2* and *cis-3*-hexene renders in all cases the terminal hydrosilane in quantitative yields with high selectivity (Table 4). This transformation likely occurs through sequential isomerization/hydrosilylation for which several authors have proved isomerization is the rate determining step.^{26, 48-50 51}

The pentacoordinated cationic Rh(III) hydride derivatives of bidentate *Si,S* ligands of general formula [HRh(SiMe₂(*o*-C₆H₄SR))(PPh₃)₂]⁺^{27, 30 48} (R = ⁱBu, Pe, Bn, ^{neo}Pe, Me), and the rigid facial derivative of a *Si,S,S*-ligand [HRh(SiMe(*o*-C₆H₄SR)₂)(PPh₃)]⁺³⁰ also selectively convert internal alkenes to linear silanes by tandem isomerization/hydrosilylation.^{27, 30, 48}

It should be noted that herein the yields and selectivities are significantly improved by the use of **Rh-1** with respect to those by the [HRh(SiMe(*o*-C₆H₄SR)₂)(PPh₃)]⁺³⁰.

On the other hand, employment of **Ir-1** as catalyst in the transformation of the same hexene isomers affords upon quantitative conversion, the allyl silane as the major product (Table 4). The selectivity to allyl silane ranged from 52-85% for the different hexene isomers. Notably *cis*- and *trans*-2-hexene have similar selectivities but there is a larger gap when converting the 3-hexene isomers. The other by-products of these reactions are vinylsilane and the terminal hydrosilane (Table S6). These conversions and selectivities are again better than those observed in the *Si,S,S*-Ir system which selectively converts internal alkenes to allylsilanes and comparable to those in the bidentate *Si,S*-Ir system with bulky substituents.³⁰ Vinylsilane formation accounts to 11-16% for the different hexene isomers while the ratio slightly drops to less than 8% using 1-octene as substrate, pointing to higher steric repulsion in the latter leading to more selective β-hydride elimination.³⁰ Allylbenzene shows the same reactivity trend upon catalysis, hydrosilylation to the terminal silane with **Rh-1** and dehydrogenative silylation to allyl silane upon use of **Ir-1** (**Scheme**). We propose **Ir-1** catalysis favors the formation of allylic over vinyl products, thus in styrene and other substrates where allylsilane generation is not possible, vinylsilanes are generated albeit upon longer times and with lower selectivities in comparison with **Rh-1** catalysis.

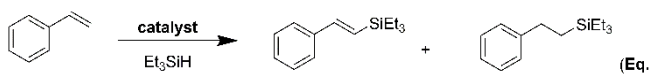
Hydrosilylation/dehydrogenative silylation occurs following an alkene isomerization process as our results indicate that both **Rh-1** and **Ir-1** are inactive in the direct Si functionalization of internal alkenes. Several mechanisms have been proposed for olefin isomerization.^{21, 50, 52} Notably the 1,2- and 1,3-hydrogen shifts⁵³ could be suggested. We postulate our system would undergo the latter allyl pathway through an inner sphere mechanism (**Scheme 3**). Our catalysts possess two vacant coordination sites which would allow for alkene coordination to the metal as in species G. The latter would subsequently undergo substitution of the chloride by the silyl group (species H). The agostic interaction of the hydrogen at the allylic position would render the η³-allyl coordinated complex I, which upon rotation and reinsertion would lead to the isomerized alkene J. This transformation would occur in internal alkenes to form terminal alkenes. The silicon functionalization that follows isomerization, again sees important differences between the use of Rh or Ir as in Scheme 2. It should be noted that the results in Table 4 are obtained in the absence of SHA (Scheme 4).

3.3 Solvent effects. Screening solvent-free conditions and toluene, dichloromethane and THF as solvents, results in similar conversions and selectivities with styrene as substrate and **Rh-1** as the catalyst (Table S3), unlike the RhCl(COD)₂/PPh₃

system which works significantly better in dioxane and THF for the dehydrogenative silylation process.³⁶ The cationic Rh(III) complex $[\text{HRh}(\kappa^3\text{-S,S,Si-SiMe}(\text{o-C}_6\text{H}_4\text{SMe})_2)(\text{PPh}_3)]^+$ leads to the anti-Markonikov hydrosilylation product of styrene under neat conditions, albeit with 48% conversion and 76% selectivity.²⁷ In our case, selectivity for the conversion of styrenes is largely enhanced by the use of CH_3CN as solvent. In contrast to the results previously discussed in toluene where dehydrogenative silylation competes with hydrosilylation by both **Rh-1** and **Ir-1**. Remarkably, the regioselectivity of styrene derivatives can be tuned in acetonitrile by the choice of metal. Indeed, the employment of **Rh-1** leads exclusively to the hydrosilylated styrene products analogous to **3** while **Ir-1** mainly leads to dehydrogenative silylation species type **2** (Table 5).

According to the mechanistic proposal in **Scheme 2**, it is expected that the weakly coordinating CH_3CN would block the available coordination site in intermediate species C thereby favoring the hydrosilylation pathway. In contrast, in the absence of coordinating solvent as in toluene, the pathway involving species D would be preferred as it would reduce the unsaturation of the metal center while forming a strong M-H bond.

Table 2. Optimization of the Rh(III) catalyzed dehydrogenative silylation of styrene with Et_3SiH .



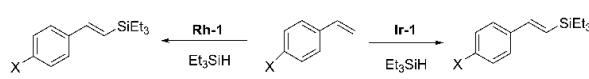
Entry	Cat	Additive	Solvent	Conv. (%) ^a	T/°C	2/3
1	Rh-1	-	Toluene	100	95	50/50
2	Rh-2	-	Toluene	100	95	48/52
3	Rh-3	-	Toluene	100	95	47/53
4	Rh-4	-	Toluene	98	95	25/75
5	Rh-5	-	DCM	100	80	52/48
6	Rh-1	-	DCM	100	80	44/56
7	Rh-1	-	THF	100	80	45/55
8	Rh-1	-	neat	100	95	44/56
9	Rh-1 ^a	nbe	Toluene	100	95	52/48
10	Rh-1 ^b	nbe	Toluene	100	95	62/38
11	Rh-1 ^c	-	Toluene	100	95	77/23
12	Rh-1 ^d	-	Toluene	100	95	90/10
13	-	-	Toluene	n.c.	95	-

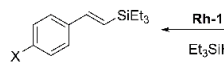
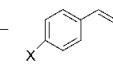
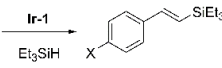
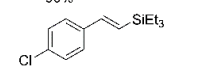
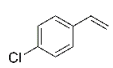
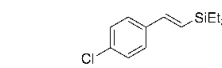
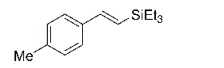
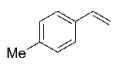
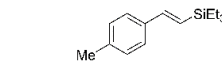
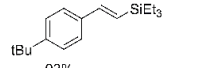
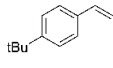
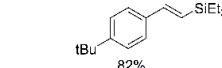
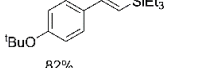
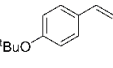
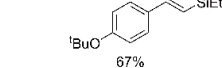
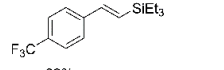
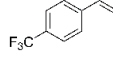
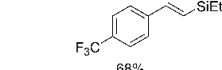
See also Table S3 in Supplementary Information. Abbreviations: nbe = norbonene; n.c. = no conversion detected. Reaction conditions: Styrene (0.2 mmol), Et_3SiH (0.2 mmol), catalyst (1 mol %), solvent (0.2 mL). Reaction times 24 h, except 5 h (entries 9, 12). DCM = dichloromethane, THF = tetrahydrofuran. [a] 2 equiv. of additive (nbe). [b] 5 equiv. of additive (nbe). [c] 2 equiv. of styrene. [d] 5 equiv. of styrene. The conversion and selectivity were determined by GC-MS and ^1H NMR with respect to Et_3SiH .

3.4 Silane effects. Different silanes were also investigated in the transformation of styrene and 1-hexene by **Rh-1**. Employment of $\text{HSi}(\text{OEt})_3$, $\text{HSiMe}(\text{OEt})_2$ or $\text{HSiMe}(\text{OSiMe}_3)_2$ and the equimolar amounts of alkenes in toluene as solvent, leads to the hydrosilylation products with excellent conversions and

selectivity (Table 6). These results should be compared to those obtained under similar conditions with HSiEt_3 , where a similar ratio of the dehydrogenative silylation/silylation products was obtained under unoptimized conditions (Table 1 and Table S3). In these new reactions, the β -hydride elimination step is disfavored while the hydrosilane formation is preferred (**Schemes 2, 3 and S2**).^{36, 54} Higher ratios of the hydrosilane with respect to the unsaturated silane have also been observed in other systems including the $[\text{RhCl}(\text{COD})]_2/\text{PPh}_3$ upon the use of $\text{HSiMe}(\text{OR})_2$.³⁶

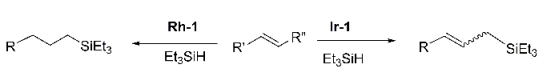
Table 3. Catalyzed reactions of substituted styrenes and Et_3SiH in toluene as solvent under optimized dehydrogenative silylation conditions.

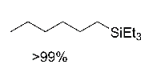
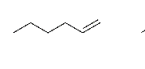
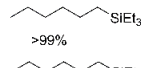
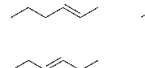
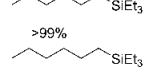
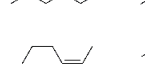
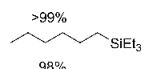
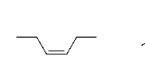
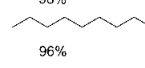
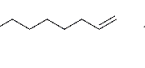
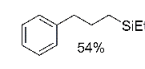
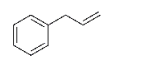
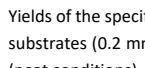
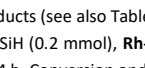


		
90%		68%
		
91%		53%
		
89%		40%
		
93%		82%
		
82%		67%
		
89%		68%

Yields of the specified products (see also Table S5 for more details). Reaction conditions: Styrene substrates (1.0 mmol), Et_3SiH (0.2 mmol), **Rh-1** or **Ir-1** (1 mol %), toluene (0.2 mL), 95 °C. Reaction time 5 h for **Rh-1**, 24 h for **Ir-1**.

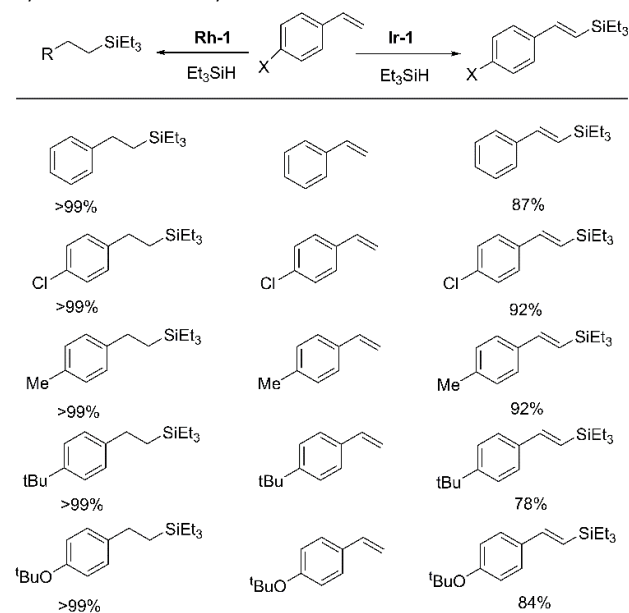
Table 4. Rh hydrosilylation versus Ir isomerization/dehydrogenative silylation of aliphatic substrates by **Rh-1** and **Ir-1** in toluene as solvent.



Isomerization-hydrosilylation	Isomerization-dehydrogenative silylation
	
>99%	(E+Z) 85%
	
>99%	(E+Z) 71%
	
>99%	(E+Z) 67%
	
>99%	(E+Z) 70%
	
98%	(E+Z) 52%
	
96%	(E+Z) 52%
	
54%	(E+Z) 70%

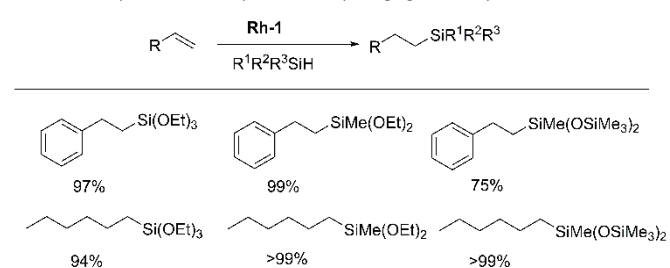
Yields of the specified products (see also Tables S5 and S6). Reaction conditions: Alkene substrates (0.2 mmol), Et_3SiH (0.2 mmol), **Rh-1** or **Ir-1** (1 mol %), no additional solvent (neat conditions), 40 °C, 24 h. Conversion and selectivity were determined by ^1H NMR.

Table 5. Tuning the selectivity of dehydrogenative silylation/hydrosilylation of styrenes in acetonitrile by the choice of metal.

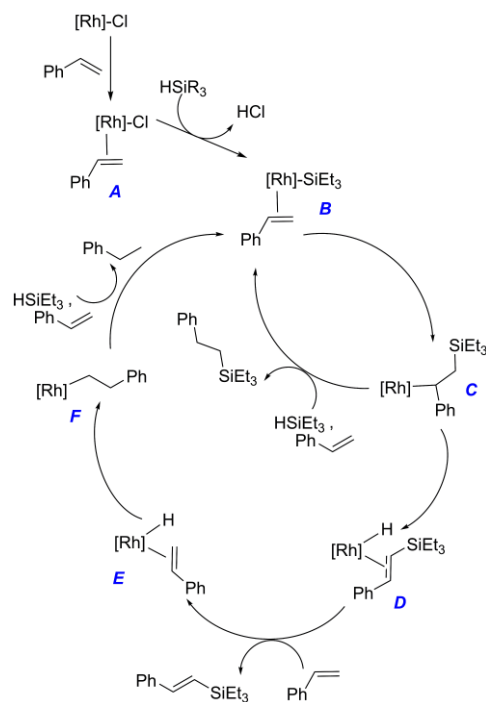


Yields of the specified products (see also SI for conversion values). Reaction conditions: Styrene substrates (0.2 mmol), Et₃SiH (0.2 mmol), **Rh-1** or **Ir-1** (1 mol %), CH₃CN (0.2 mL), 80 °C for 24 h. Conversion and selectivity were determined by GC-MS and ¹H NMR.

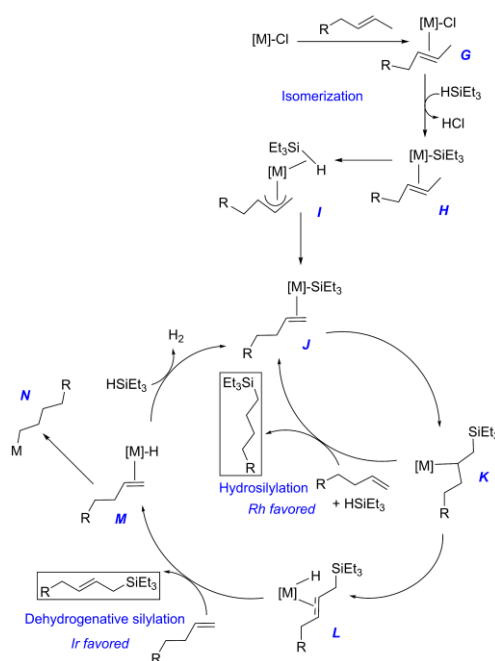
Table 6. Alkoxy silane and siloxy silanes as silylating agents of styrene and 1-hexene.



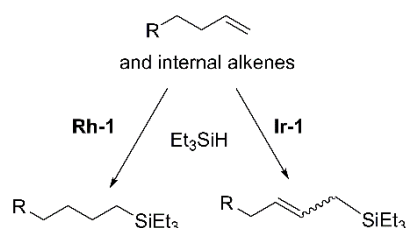
Yields of the specified products (see also Table S7). Reaction conditions: alkene substrates (0.2 mmol), alkoxy silane or siloxy silane (0.2 mmol), **Rh-1** (1 mol %), toluene (0.2 mL), 95 °C for 24 h. Conversion and selectivity determined by GC-MS.



Scheme 2. The proposed mechanism for the dehydrogenative silylation/hydrosilylation of styrene by the 14-electron **Rh-1** in toluene.



Scheme 3. The proposed mechanism for the tandem isomerization-dehydrogenative silylation and isomerization-hydrosilylation of aliphatic alkenes by **Rh-1** and **Ir-1** in toluene.



Scheme 4. The different outcomes of terminal and remote alkenes upon **Rh-1** or **Ir-1** catalysis.

Conclusions

In conclusion, we have isolated a family of four-coordinated 14-electron sawhorse Rh(III) complexes bearing a tridentate semirigid bis(silyl)-*o*-tolylphosphine ligand with isopropyl substituents on the Si atoms. All five complexes display a sawhorse geometry around Rh and exhibit very similar spectroscopic and structural properties despite the fourth ligand spanning from Cl (**Rh-1**) to Br (**Rh-2**) to I (**Rh-3**) to triflate (**Rh-4**). The structure is even preserved in **Rh-5**, the GaCl₃ μ₁-adduct of **Rh-1**. Complexes **Rh-1** and **Ir-1**, efficiently catalyze the challenging Si functionalization of alkenes offering the option of tunability depending on the identity of the metal center and solvent employed.

Complex **Rh-1** catalyzes the dehydrogenative silylation of styrene with Et₃SiH in toluene while it leads to hydrosilylation products in acetonitrile. **Rh-1** is also an excellent catalyst in the sequential isomerization/hydrosilylation of terminal and remote aliphatic alkenes with Et₃SiH, leading efficiently and selectively to the terminal anti-Markonikov hydrosilylation product. With aliphatic alkenes, no hydrogenation products are observed. Complementary, catalysis of the same hexene isomers by **Ir-1** renders allyl silanes, the tandem isomerization/dehydrogenative silylation products.

Experimental section

General considerations

Experiments were performed under argon atmosphere using standard Schlenk methods or in an MBraun glove box unless stated otherwise. Laboratory solvents were dried and purified over MBraun column systems. Benzene-d₆ and CDCl₃ were passed through a Pasteur pipette containing molecular sieves and basic alumina and then degassed via three freeze–pump–thaw cycles and stored over molecular sieves. [MCl{κ³(P,Si,Si)PPh(o-C₆H₄CH₂SiⁱPr₂)₂}⁵⁰] (M = Rh, **Rh-1** and M = Ir, **Ir-1**) were synthesized according to the reported procedure.¹¹ The other reagents were purchased from Sigma Aldrich and used as received. Nuclear magnetic resonance (NMR) experiments were performed on a Bruker Avance 300, 500 and 600 spectrometers. All chemical shifts (δ) for ¹H, ²⁹Si and ¹³C are relative to TMS and are reported in parts per million (ppm). GC-MS analyses were performed on a GC MS-QP2010S instrument.

Synthesis of [RhBr{κ³(P,Si,Si)PPh(o-C₆H₄CH₂SiⁱPr₂)₂}] (**Rh-2**)

In a Schlenk flask, equimolar amounts of **Rh-1** (30 mg, 0.046 mmol) and NaBr (4.7 mg, 0.046 mmol) were dissolved in 2 mL of dry THF. The resulted yellow solution was left stirring for 24 hours. It was subsequently filtered through celite and the volatiles were removed under vacuum, the crude solid was washed with 3 portions of 1 mL of dry pentane and dried in vacuum for 6 hours. Complex **Rh-2** was obtained as a yellow solid in 93% yield (30 mg). Crystals suitable for X ray diffraction were grown from C₆D₆/CH₂Cl₂ solutions. Anal. Calcd. for C₃₂H₄₅RhBrPSi₂·0.67CH₂Cl₂: C: 51.87%, H: 6.17%; Found: C:51.85%, H:6.43%. ¹H NMR (500 MHz, C₆D₆): δ 7.59 – 7.56 (m, 2H, CH_{arom}), 7.00 (q, *J*_{HH} = 6.1 Hz, *J*_{HH} = 4.8 Hz, 5H, CH_{arom}), 6.94 – 6.89 (m, 4H, CH_{arom}), 6.74 (t, *J*_{HH} = 7.4 Hz, 2H, CH_{arom}), 2.24, 2.12 (AB pattern, *J*_{AB} = 14.7 Hz: 2.24 (dd, ²*J*_{HH} = 14.7, ³*J*_{HH} = 5.9, 2H, CH₂), 2.12 (d, ²*J*_{HH} = 14.7 Hz, 2H, CH₂), 1.80 (sept, ²*J*_{HH} = 7.4 Hz, 2H, CH-ⁱPr), 1.70 (sept, ²*J*_{HH} = 7.4 Hz, 2H, CH-ⁱPr), 1.59 (d, ²*J*_{HH} = 7.4 Hz, 6H, CH₃-ⁱPr), 1.16 (d, ²*J*_{HH} = 7.4 Hz, 6H, CH₃-ⁱPr), 0.94 (dd, ²*J*_{HH} = 10 Hz, ³*J*_{HH} = 7.4 Hz, 12H, CH₃-ⁱPr) ppm. ¹³C{¹H} NMR (150.9 MHz, C₆D₆): 146.69 (d, *J*_{CP} = 14.2 Hz, C_{ipso}), 134.18 (d, *J*_{CP} = 11.1 Hz, CH_{arom}), 132.45 (d, *J*_{CP} = 5.0 Hz, CH_{arom}), 131.76 (d, *J*_{CP} = 8.1 Hz, CH_{arom}), 131.19 (d, *J*_{CP} = 2.3 Hz, CH_{arom}), 131.00 (d, *J*_{CP} = 2.1 Hz, CH_{arom}), 130.53 (d, *J*_{CP} = 49.3 Hz, C_{ipso}), 129.31 (d, *J*_{CP} = 10.0 Hz, CH_{arom}), 126.84 (d, *J*_{CP} = 55.2 Hz, C_{ipso}), 125.48 (d, *J*_{CP} = 8.4 Hz, CH_{arom}), 23.40 (d, *J*_{CP} = 17.7 Hz, CH₂), 21.65 (s, CH₃-ⁱPr), 21.63 (s, CH-ⁱPr), 20.74 (s, CH₃-ⁱPr), 20.10 (s, CH₃-ⁱPr), 18.94 (s, CH₃-ⁱPr), 18.88 (t, |*J*_{CP} + *J*_{CRH}| = 1.5 Hz, CH-ⁱPr) ppm. ³¹P{¹H} NMR (202.46 MHz, C₆D₆): 31.77 (d, *J*_{PRh} = 148.6, *J*_{PSi} = 13 Hz) ppm. DEPT ²⁹Si{¹H} NMR (99.36 MHz, C₆D₆): 75.6 (dd, *J*_{Si-Rh} = 38.3, *J*_{Si-P} = 13 Hz) ppm.

Synthesis of [RhI{κ³(P,Si,Si)PPh(o-C₆H₄CH₂SiⁱPr₂)₂}] (**Rh-3**)

In a Schlenk flask, 30 mg (0.046 mmol) of **Rh-1** and 6.9 mg of NaI (0.046 mmol) were dissolved in 2 mL of dry THF. The resulted yellow solution was left stirring for 24 hours at room temperature. After this time, the reaction mixture was filtered through celite and the volatiles were removed under vacuum. The crude was washed three times with portions of 1 mL of dry pentane and dried in vacuum for 6 hours. Complex **Rh-3** was obtained as a pale-yellow solid in 94% yield (32 mg). Crystals suitable for X ray diffraction were grown from concentrated C₆D₆ solutions at room temperature. Anal. Calcd. for C₃₂H₄₅RhIPSi₂: C: 51.48%, H: 6.07%; Found: C: 51.79%, H: 6.22%. ¹H NMR (500 MHz, C₆D₆, 298 K): δ 7.63 – 7.54 (m, 2H, CH_{arom}), 7.04 – 6.89 (m, 9H, CH_{arom}), 6.78 – 6.70 (m, 2H, CH_{arom}); 2.22, 2.12 (AB pattern, *J*_{AB} = 14.8 Hz: 2.22 (ddd, ²*J*_{HH} = 14.8, ³*J*_{HH} = 6.9, ⁴*J*_{HP} = 1.9 Hz, 2H, CH₂), 2.12 (d, ²*J*_{HH} = 14.8 Hz, 2H, CH₂), 1.76 (sept, ²*J*_{HH} = 7.5 Hz 2H, CH-ⁱPr), 1.72 (sept, ²*J*_{HH} = 7.5 Hz 2H, CH-ⁱPr), 1.59 (d, ²*J*_{HH} = 7.4 Hz, 6H, CH₃-ⁱPr), 1.21 (d, ²*J*_{HH} = 7.7 Hz, 6H, CH₃-ⁱPr), 0.93 (d, ²*J*_{HH} = 7.4 Hz, 6H, CH₃-ⁱPr), 0.87 (d, ²*J*_{HH} = 7.5 Hz, 6H, CH₃-ⁱPr) ppm. ¹³C{¹H} NMR (150.9 MHz, C₆D₆): 146.77 (d, *J*_{CP} = 14.4 Hz, C_{ipso}), 133.90 (d, *J*_{CP} = 10.8 Hz, CH_{arom}), 132.66 (d, *J*_{CP} = 4.9 Hz, CH_{arom}), 131.85 (d, *J*_{CP} = 8.1 Hz, CH_{arom}), 131.18 (d, *J*_{CP} = 2.5 Hz, CH_{arom}), 130.90 (d, *J*_{CP} = 2.7 Hz, CH_{arom}), 129.82 (d, *J*_{CP} = 48.8 Hz, C_{ipso}), 129.26 (d, *J*_{CP} = 10.0 Hz, CH_{arom}), 126.47 (d, *J*_{CP} = 55.1 Hz, C_{ipso}), 125.49 (d, *J*_{CP} = 8.2 Hz, CH_{arom}), 23.54 (d,

$J_{CP} = 18.4$ Hz, CH₂), 22.41 (s, CH₃-^{*i*}Pr), 21.20 (s, CH-^{*i*}Pr), 20.82 (s, CH₃-^{*i*}Pr), 19.99 (s, CH₃-^{*i*}Pr), 19.35 (t, $|J_{CP} + J_{CRh}| = 1.9$ Hz, CH-^{*i*}Pr), 19.02 (s, CH₃-^{*i*}Pr) ppm. ³¹P{¹H} NMR (202.46 MHz, C₆D₆): 30.90 (d, $J_{PRh} = 147.4$, $J_{PSi} = 12$ Hz) ppm. DEPT ²⁹Si{¹H} NMR (99.36 MHz, C₆D₆): 75.77 (dd, $J_{Si-Rh} = 37.0$, $J_{Si-P} = 12$ Hz) ppm.

Synthesis of [RhOTf{κ³(P,Si,Si) PPh(o-C₆H₄CH₂Si^{*i*}Pr₂)₂] (Rh-4)

In a Schlenk flask, 30 mg (0.046 mmol) of Rh-1 and 23.5 mg of AgOTf (0.092 mmol) were dissolved in 2 mL of dry toluene. The resulted brown solution was left stirring for 24 hours at room temperature in the dark. The solution was filtered through celite and the volatiles were removed under the vacuum, the crude was washed with 3 portions of 1 mL of dry pentane and dried in vacuum for 6 hours. Complex Rh-4 was obtained as an orange viscous compound in 66% yield (23 mg). Crystals suitable for X ray diffraction were grown from concentrated C₆D₆ solutions at room temperature. ¹H NMR (500 MHz, C₆D₆): δ 7.64 (ddd, $J_{HH} = 11.3$ Hz, $J_{HH} = 7.9$ Hz, $J_{HP} = 1.6$ Hz 2H, CH_{arom}), 7.09–7.03 (m, 3H, CH_{arom}), 6.98–6.82 (m, 6H, CH_{arom}), 6.70 (tt, $J_{HH} = 7.4$ Hz, $J_{HP} = 1.6$ Hz 2H, CH_{arom}), 2.25, 2.05 (AB pattern, $J_{AB} = 15.2$ Hz: 2.25 (ddd, $^2J_{HH} = 15.2$, $^3J_{HH} = 5.8$, $^4J_{HP} = 2.5$ 2H, CH₂), 2.05 (d, $^2J_{HH} = 15.2$ Hz, 2H, CH₂), 1.83 (sept, $^2J_{HH} = 7.5$ Hz, 2H, CH-^{*i*}Pr), 1.65 (sept, $^2J_{HH} = 7.7$ Hz, 2H, CH-^{*i*}Pr), 1.45 (d, $^2J_{HH} = 7.5$ Hz, 6H, CH₃-^{*i*}Pr), 1.08 (d, $^2J_{HH} = 7.3$ Hz, 6H, CH₃-^{*i*}Pr), 0.94 (pseudo dd, $^2J_{HH} = 7.5$ Hz, $^3J_{HH} = 4.7$ Hz, 12H, CH₃-^{*i*}Pr) ppm. ¹³C{¹H} NMR (125.76 MHz, C₆D₆): 145.83 (d, $J_{CP} = 13.5$ Hz, C_{ipso}), 134.44 (d, $J_{CP} = 10.8$ Hz, CH_{arom}), 132.76 (d, $J_{CP} = 5.9$ Hz, CH_{arom}), 131.99 (d, $J_{CP} = 8.4$ Hz, CH_{arom}), 131.75 (dd, $J_{CP} = 6.2$, 2.6 Hz, CH_{arom}), 129.61 (d, $J_{CP} = 10.6$ Hz, CH_{arom}), 126.17 (d, $J_{CP} = 60.3$ Hz, C_{ipso}), 125.68 (d, $J_{CP} = 2.1$ Hz, CH_{arom}), 21.83 (d, $J_{CP} = 14.6$ Hz, CH₂), 21.57 (s, CH₃-^{*i*}Pr), 20.73 (s, CH-^{*i*}Pr), 19.09 (s, CH₃-^{*i*}Pr), 18.67 (s, CH₃-^{*i*}Pr), 18.18 (s, CH₃-^{*i*}Pr), 17.00 (t, $|J_{CP} + J_{CRh}| = 1.5$ Hz, CH-^{*i*}Pr) ppm. ³¹P{¹H} NMR (202.46 MHz, C₆D₆): 37.67 (d, $J_{PRh} = 169.5$, $J_{PSi} = 15$ Hz) ppm. DEPT ²⁹Si{¹H} NMR (99.36 MHz, C₆D₆): 73.82 (dd, $J_{Si-Rh} = 38.4$, $J_{Si-P} = 15$ Hz) ppm.

Synthesis of [Rh{κ³(P,Si,Si)PPh(o-C₆H₄CH₂Si^{*i*}Pr₂)₂}ClGaCl₃] (Rh-5)

In a Schlenk flask, 30 mg (0.046 mmol) of Rh-1 and 8.1 mg of GaCl₃ (0.046 mmol) were dissolved in 2 mL of dry benzene. The resulted yellow solution was left stirring for 24 hours. The volatiles were removed under the vacuum; the crude was washed with 3 portions of 1 mL of dry pentane and dried in vacuum for 6 hours. Complex Rh-5 was obtained as a yellow-brown solid in 75% yield (29 mg). Crystals suitable for X ray diffraction were grown from concentration CDCl₃ solutions. Anal. Calcd. for C₃₂H₄₅Cl₄GaRhPSi₂·0.37CDCl₃: C: 44.39%, H: 5.26%; Found: C:44.45%, H:5.33%.

¹H NMR (500 MHz, CDCl₃): δ 7.50–7.36 (m, 4H, CH_{arom}), 7.33 (t, $J_{HH} = 7.6$ Hz, 2H, CH_{arom}), 7.22 (t, $J_{HH} = 6.4$ Hz, 2H, CH_{arom}), 7.15 (s, 1H, CH_{arom}), 7.05 (t, $J_{HH} = 7.7$ Hz, 2H, CH_{arom}), 2.21, 2.06 (AB pattern, $J_{AB} = 14.8$ Hz: 2.21 (dd, $^2J_{HH} = 15.0$, $^3J_{HH} = 4.7$, 2H, CH₂), 2.06 (d, $^2J_{HH} = 14.8$ Hz, 2H, CH₂), 1.60 (sept, $^2J_{HH} = 7.5$ Hz, 2H, CH-^{*i*}Pr), 1.30 (sept, $^2J_{HH} = 7.3$ Hz, 2H, CH-^{*i*}Pr), 1.11 (d, $^2J_{HH} = 7.3$ Hz, 6H, CH₃-^{*i*}Pr), 0.92 (d, $^2J_{HH} = 7.4$ Hz, 6H, CH₃-^{*i*}Pr), 0.84 (d, $^2J_{HH} = 7.2$ Hz, 6H, CH₃-^{*i*}Pr), 0.67 (d, $^2J_{HH} = 7.3$ Hz, 6H, CH₃-^{*i*}Pr) ppm. ¹³C{¹H} NMR (125.758 MHz, CDCl₃): 145.89 (d, $J_{CP} = 13.1$ Hz, C_{ipso}), 134.65 (d, $J_{CP} = 10.9$ Hz, CH_{arom}), 132.64 (d, $J_{CP} = 5.8$

Hz, CH_{arom}), 131.75 (d, $J_{CP} = 8.4$ Hz, CH_{arom}), 129.65 (d, $J_{CP} = 10.7$ Hz, CH_{arom}), 127.36 (d, $J_{CP} = 53.2$ Hz, C_{ipso}), 125.89 (d, $J_{CP} = 9.3$ Hz, CH_{arom}), 125.04 (d, $J_{CP} = 60.0$ Hz, C_{ipso}), 21.95 (s, CH₃-^{*i*}Pr), 21.88 (d, $J_{CP} = 12.4$ Hz, CH₂), 20.75 (s, CH-^{*i*}Pr), 19.91 (s, CH₃-^{*i*}Pr), 19.89 (s, CH₃-^{*i*}Pr), 18.96 (s, CH₃-^{*i*}Pr), 18.21 (t, $|J_{CP} + J_{CRh}| = 1.8$ Hz, CH-^{*i*}Pr) ppm. ³¹P{¹H} NMR (202.46 MHz, CDCl₃): 34.80 (d, $J_{PRh} = 177.6$) ppm. DEPT ²⁹Si{¹H} NMR (99.36 MHz, CDCl₃): 78.42 (dd, $J_{Si-Rh} = 37.3$, $J_{Si-P} = 12.6$ Hz) ppm.

Catalytic conditions. Conditions and details of the catalytic experiments as well as complete tables are provided in the Supplementary Information.

Conflicts of interest

There are no conflicts to declare.

Acknowledgements

We thank the Department of Chemistry at Mississippi State University and NSF (CHE 2102689) for financial support of this work. Mississippi Center for Supercomputing Research is acknowledged for computing resources. We also thank CONACyT-Mexico (274001) for a PhD studentship and travel grant for J.Z.M. to perform research at Mississippi State.

Notes and references

1. C. Werle, C. Bailly, L. Karmazin-Brelot, X. F. Le Goff, M. Pfeffer and J. P. Djukic, "First stabilization of 14-electron rhodium(I) complexes by hemichelation," *Angew Chem Int Ed Engl*, 2014, **53**, 9827-31.
2. H. Urtel, C. Meier, F. Eisenträger, F. Rominger, J. P. Joschek and P. Hofmann, "A Neutral Three-Coordinate Alkylrhodium(I) Complex: Stabilization of a 14-Electron Species by γ-C-H Agostic Interactions with a Saturated Hydrocarbon Group," *Angewandte Chemie International Edition*, 2001, **40**, 781-784.
3. A. B. Chaplin, "Rhodium(I) Complexes of the Conformationally Rigid IBioxMe₄ Ligand: Isolation of a Stable Low-Coordinate T-Shaped Complex," *Organometallics*, 2014, **33**, 624-626.
4. A. B. Chaplin, A. I. Poblador-Bahamonde, H. A. Sparkes, J. A. K. Howard, S. A. Macgregor and A. S. Weller, "Alkyl dehydrogenation in a Rh(i) complex via an isolated agostic intermediate," *Chemical Communications*, 2009, 10.1039/B816739G, 244-246.
5. A. C. Cooper, E. Clot, J. C. Huffman, W. E. Streib, F. Maseras, O. Eisenstein and K. G. Caulton, "Computational and Experimental Test of Steric Influence on Agostic Interactions: A Homologous Series for Ir(III)," *Journal of the American Chemical Society*, 1999, **121**, 97-106.

6. T. Komuro, K. Furuyama, T. Kitano and H. Tobita, "Synthesis of a 14-electron iridium(III) complex with a xanthene-based bis(silyl) chelate ligand (xantsil): A distorted seesaw-shaped four-coordinate geometry and reactions leading to 16-electron complexes," *Journal of Organometallic Chemistry*, 2014, **751**, 686-694.
7. R. Dorta, E. D. Stevens and S. P. Nolan, "Double C–H Activation in a Rh–NHC Complex Leading to the Isolation of a 14-Electron Rh(III) Complex," *Journal of the American Chemical Society*, 2004, **126**, 5054-5055.
8. T. M. Douglas, A. B. Chaplin and A. S. Weller, "Dihydrogen Loss from a 14-Electron Rhodium(III) Bis-Phosphine Dihydride To Give a Rhodium(I) Complex That Undergoes Oxidative Addition with Aryl Chlorides," *Organometallics*, 2008, **27**, 2918-2921.
9. N. Phillips, J. Rowles, M. J. Kelly, I. Riddlestone, N. H. Rees, A. Dervisi, I. A. Fallis and S. Aldridge, "Sterically Encumbered Iridium Bis(N-heterocyclic carbene) Complexes: Air-Stable 14-Electron Cations and Facile Degenerate C–H Activation," *Organometallics*, 2012, **31**, 8075-8078.
10. R. Dorta, R. Goikhman and D. Milstein, "Reactivity of [Ir(COE)₂(solvent)₂]PF₆ Complexes toward Alkylphosphines: Room-Temperature C–H Activation (Cyclometalation) and Isolation of a 14-Electron Alkyl–Iridium(III) Complex," *Organometallics*, 2003, **22**, 2806-2809.
11. M. V. Corona-González, J. Zamora-Moreno, M. A. Muñoz-Hernández, L. Vendier, S. Sabo-Etienne and V. Montiel-Palma, "Exploiting the Versatility of Phosphinobenzylsilanes for the Stabilization of 14-Electron Rhodium(III) and Iridium(III) Complexes," *European Journal of Inorganic Chemistry*, 2019, **2019**, 1854-1858.
12. S. Gorla, M. L. Díaz-Ramírez, N. S. Abeynayake, D. M. Kaphan, D. R. Williams, V. Martis, H. A. Lara-García, B. Donnadieu, N. Lopez, I. A. Ibarra and V. Montiel-Palma, "Functionalized NU-1000 with an Iridium Organometallic Fragment: SO₂ Capture Enhancement," *ACS Applied Materials & Interfaces*, 2020, **12**, 41758-41764.
13. M. V. Corona-González, J. Zamora-Moreno, C. A. Cuevas-Chávez, E. Rufino-Felipe, E. Mothes-Martin, Y. Coppel, M. A. Muñoz-Hernández, L. Vendier, M. Flores-Alamo, M. Grellier, S. Sabo-Etienne and V. Montiel-Palma, "A family of rhodium and iridium complexes with semirigid benzylsilyl phosphines: from bidentate to tetradentate coordination modes," *Dalton Transactions*, 2017, **46**, 8827-8838.
14. L. Abis, R. Santi and J. Halpern, "Synthesis and characterization of some trans-hydridomethylbis(phosphine)-platinum(II) and -palladium(II) complexes," *Journal of Organometallic Chemistry*, 1981, **215**, 263-267.
15. C. Romano, D. Fiorito and C. Mazet, "Remote Functionalization of α,β -Unsaturated Carbonyls by Multimetallic Sequential Catalysis," *J. Am. Chem. Soc.*, 2019, **141**, 16983-16990.
16. M. Brookhart, M. L. H. Green and G. Parkin, "Agostic interactions in transition metal compounds," *Proceedings of the National Academy of Sciences*, 2007, **104**, 6908-6914.
17. In complex Rh-2, the shortest contacts are Rh...H26B 2.716 Å and Rh...C26 3.313 Å. In Rh-3, Rh-H28E 2.897 Å and Rh-C28B 3.454 Å. In complex Rh-4, Rh...H32 2.557 Å, Rh...C32 3.203 Å. In Rh-5, Rh...H23B 2.992 Å, Rh...C23 3.589 Å. In all these cases, the distances involve a methyl hydrogen from the isopropyl substituents on Si.
18. C. A. Cuevas-Chávez, L. Vendier, S. Sabo-Etienne and V. Montiel-Palma, "Iridium complexes featuring a tridentate SiPSi ligand: from dimeric to monomeric 14, 16 or 18-electron species," *Dalton Transactions*, 2019, **48**, 14010-14018.
19. X. Jia and Z. Huang, "Conversion of alkanes to linear alkylsilanes using an iridium-iron-catalysed tandem dehydrogenation-isomerization-hydrosilylation," *Nat Chem*, 2016, **8**, 157-61.
20. C. C. H. Atienza, T. Diao, K. J. Weller, S. A. Nye, K. M. Lewis, J. G. P. Delis, J. L. Boyer, A. K. Roy and P. J. Chirik, "Bis(imino)pyridine Cobalt-Catalyzed Dehydrogenative Silylation of Alkenes: Scope, Mechanism, and Origins of Selective Allylsilane Formation," *Journal of the American Chemical Society*, 2014, **136**, 12108-12118.
21. A. Vasseur, J. Bruffaerts and I. Marek, "Remote functionalization through alkene isomerization," *Nature Chemistry*, 2016, **8**, 209-219.
22. D. Noda, A. Tahara, Y. Sunada and H. Nagashima, "Non-Precious-Metal Catalytic Systems Involving Iron or Cobalt Carboxylates and Alkyl Isocyanides for Hydrosilylation of Alkenes with Hydrosiloxanes," *Journal of the American Chemical Society*, 2016, **138**, 2480-2483.
23. C. Chen, M. B. Hecht, A. Kavara, W. W. Brennessel, B. Q. Mercado, D. J. Weix and P. L. Holland, "Rapid, Regioconvergent, Solvent-Free Alkene Hydrosilylation with a Cobalt Catalyst," *Journal of the American Chemical Society*, 2015, **137**, 13244-13247.
24. V. Srinivas, Y. Nakajima, W. Ando, K. Sato and S. Shimada, "(Salicylaldiminato)Ni(ii)-catalysts for hydrosilylation of olefins," *Catalysis Science & Technology*, 2015, **5**, 2081-2084.
25. I. Buslov, F. Song and X. Hu, "An Easily Accessed Nickel Nanoparticle Catalyst for Alkene Hydrosilylation with Tertiary Silanes," *Angewandte Chemie International Edition*, 2016, **55**, 12295-12299.
26. R. Srivastava, M. Jakoobi, C. Thieuleux, E. A. Quadrelli and C. Camp, "A family of rhodium(i) NHC chelates featuring O-containing

- tethers for catalytic tandem alkene isomerization–hydrosilylation," *Dalton Transactions*, 2021, **50**, 869-879.
27. S. Azpeitia, M. A. Garralda and M. A. Huertos, "Rhodium(III) catalyzed solvent-free tandem isomerization-hydrosilylation from internal alkenes to linear silanes," *ChemCatChem*, 2017, **9**, 1901-1905.
28. S. Azpeitia, A. Rodriguez-Dieguez, M. A. Garralda and M. A. Huertos, "From Remote Alkenes to Linear Silanes or Allylsilanes depending on the Metal Center," *ChemCatChem*, 2018, **10**, 2210-2213.
29. M. Jakoobi, V. Dardun, L. Veyre, V. Meille, C. Camp and C. Thieuleux, "Developing a Highly Active Catalytic System Based on Cobalt Nanoparticles for Terminal and Internal Alkene Hydrosilylation," *J. Org. Chem.*, 2020, **85**, 11732-11740.
30. S. Azpeitia, A. Rodriguez-Dieguez, M. A. Garralda and M. A. Huertos, "From Remote Alkenes to Linear Silanes or Allylsilanes depending on the Metal Center," *ChemCatChem*, 2018, **10**, 2210-2213.
31. T. Komiyama, Y. Minami and T. Hiyama, "Recent Advances in Transition-Metal-Catalyzed Synthetic Transformations of Organosilicon Reagents," *ACS Catalysis*, 2017, **7**, 631-651.
32. S. E. Denmark and J. D. Baird, "Palladium-Catalyzed Cross-Coupling Reactions of Silanolates: A Paradigm Shift in Silicon-Based Cross-Coupling Reactions," *Chemistry – A European Journal*, 2006, **12**, 4954-4963.
33. B. Marciniec, "Catalysis by transition metal complexes of alkene silylation—recent progress and mechanistic implications," *Coordination Chemistry Reviews*, 2005, **249**, 2374-2390.
34. J. V. Obligacion and P. J. Chirik, "Earth-abundant transition metal catalysts for alkene hydrosilylation and hydroboration," *Nature Reviews Chemistry*, 2018, **2**, 15-34.
35. Y. Gao, L. Wang and L. Deng, "Distinct Catalytic Performance of Cobalt(I)–N-Heterocyclic Carbene Complexes in Promoting the Reaction of Alkene with Diphenylsilane: Selective 2,1-Hydrosilylation, 1,2-Hydrosilylation, and Hydrogenation of Alkene," *ACS Catalysis*, 2018, **8**, 9637-9646.
36. W. Lu, C. Li, X. Wu, X. Xie and Z. Zhang, "[Rh(COD)Cl]₂/PPh₃-Catalyzed Dehydrogenative Silylation of Styrene Derivatives with NBE as a Hydrogen Acceptor," *Organometallics*, 2020, **39**, 3780-3788.
37. G. Albertin, S. Antoniutti, M. Bedin, J. Castro and S. Garcia-Fontán, "Synthesis and Characterization of Triazenide and Triazene Complexes of Ruthenium and Osmium," *Inorganic Chemistry*, 2006, **45**, 3816-3825.
38. P. B. Hitchcock, A. G. Hulkes, M. F. Lappert and A. V. Protchenko, "Diversity of triflate coordination modes in neodymocene complexes containing bulky bis(trimethylsilyl)cyclopentadienyl ligands," *Inorg. Chim. Acta*, 2006, **359**, 2998-3006.
39. G. Albertin, S. Antoniutti, A. Bacchi, M. Bergamo, E. Bordignon and G. Pelizzi, "Mono- and Bis(hydrazine) Complexes of Osmium(II): Synthesis, Reactions, and X-ray Crystal Structure of the [Os(NH₂NH₂)₂{P(OEt)₃}₄](BPh₄)₂ Derivative," *Inorganic Chemistry*, 1998, **37**, 479-489.
40. E. Peris, "Smart N-Heterocyclic Carbene Ligands in Catalysis," *Chemical Reviews*, 2018, **118**, 9988-10031.
41. G. Mancano, M. J. Page, M. Bhadbhade and B. A. Messerle, "Hemilabile and Bimetallic Coordination in Rh and Ir Complexes of NCN Pincer Ligands," *Inorganic Chemistry*, 2014, **53**, 10159-10170.
42. M. Aliaga-Lavrijsen, M. Iglesias, A. Cebollada, K. Garcés, N. García, P. J. Sanz Miguel, F. J. Fernández-Alvarez, J. J. Pérez-Torrente and L. A. Oro, "Hydrolysis and Methanolysis of Silanes Catalyzed by Iridium(III) Bis-N-Heterocyclic Carbene Complexes: Influence of the Wingtip Groups," *Organometallics*, 2015, **34**, 2378-2385.
43. C. Verries-Peylhard, "Synthesis, Raman spectrum and crystal structure of copper(II) tetrachlorogallate," *C. R. Seances Acad. Sci., Ser. 2*, 1982, **295**, 171-4.
44. R. Takeuchi and N. Tanouchi, "Complete reversal of stereoselectivity in rhodium complex-catalysed hydrosilylation of alk-1-yne," *Journal of the Chemical Society, Chemical Communications*, 1993, 10.1039/C39930001319, 1319-1320.
45. A. Bokka and J. Jeon, "Regio- and Stereoselective Dehydrogenative Silylation and Hydrosilylation of Vinylarenes Catalyzed by Ruthenium Alkylidenes," *Org. Lett.*, 2016, **18**, 5324-5327.
46. R. Takeuchi and H. Yasue, "Cationic Rhodium Complex-Catalyzed Highly Selective Dehydrogenative Silylation of Styrene," *Organometallics*, 1996, **15**, 2098-2102.
47. F. Kakiuchi, K. Nogami, N. Chatani, Y. Seki and S. Murai, "Dehydrogenative silylation of 1,5-dienes with hydrosilanes catalyzed by RhCl(PPh₃)₃," *Organometallics*, 1993, **12**, 4748-4750.

48. U. Prieto, S. Azpeitia, E. S. Sebastian, Z. Freixa, M. A. Garralda and M. A. Huertos, "Steric Effects in the Catalytic Tandem Isomerization-Hydrosilylation Reaction," *ChemCatChem*, 2021, **13**, 1403-1409.

49. I. Buslov, J. Because, S. Mazza, M. Montandon-Clerc and X. Hu, "Chemoselective Alkene Hydrosilylation Catalyzed by Nickel Pincer Complexes," *Angewandte Chemie International Edition*, 2015, **54**, 14523-14526.

50. H. Sommer, I. Marek, F. Julia-Hernandez, R. Martin and R. Martin, "Walking Metals for Remote Functionalization," *ACS Cent Sci*, 2018, **4**, 153-165.

51. H. Sommer, F. Julia-Hernandez, R. Martin and I. Marek, "Walking Metals for Remote Functionalization," *ACS Cent. Sci.*, 2018, **4**, 153-165.

52. D. Kim, G. Pillon, D. J. DiPrimio and P. L. Holland, "Highly Z-Selective Double Bond Transposition in Simple Alkenes and Allylarenes through a Spin-Accelerated Allyl Mechanism," *Journal of the American Chemical Society*, 2021, **143**, 3070-3074.

53. S. Biswas, Z. Huang, Y. Choliy, D. Y. Wang, M. Brookhart, K. Krogh-Jespersen and A. S. Goldman, "Olefin Isomerization by Iridium Pincer Catalysts. Experimental Evidence for an η^3 -Allyl Pathway and an Unconventional Mechanism Predicted by DFT Calculations," *Journal of the American Chemical Society*, 2012, **134**, 13276-13295.

54. T. Lee and J. F. Hartwig, "Mechanistic Studies on Rhodium-Catalyzed Enantioselective Silylation of Aryl C-H Bonds," *Journal of the American Chemical Society*, 2017, **139**, 4879-4886.